JCB Article

Reversed polarized delivery of an aquaporin-2 mutant causes dominant nephrogenic diabetes insipidus

Erik-Jan Kamsteeg,[1] Daniel G. Bichet,[2] Irene B.M. Konings,[1] Hubert Nivet,[3] Michelle Lonergan,[2] Marie-Françoise Arthus,[2] Carel H. van Os,[1] and Peter M.T. Deen[1]

[1]Department of Physiology, Nijmegen Center for Molecular Life Sciences, University Medical Center Nijmegen, Nijmegen 6500 HB, Netherlands
[2]Faculté de Médecine, Université de Montréal et Centre de Recherches, Hôpital du Sacre-Coeur de Montréal, H4J-1C5 Montréal, Quebec, Canada
[3]Département de Nephrology, Centre Hospitalier Universitaire de Tours, 37044 Tours, France

Vasopressin regulates body water conservation by redistributing aquaporin-2 (AQP2) water channels from intracellular vesicles to the apical surface of renal collecting ducts, resulting in water reabsorption from urine. Mutations in *AQP2* cause autosomal nephrogenic diabetes insipidus (NDI), a disease characterized by the inability to concentrate urine. Here, we report a frame-shift mutation in *AQP2* causing dominant NDI. This AQP2 mutant is a functional water channel when expressed in *Xenopus* oocytes. However, expressed in polarized renal cells, it is misrouted to the basolateral instead of apical plasma membrane. Additionally, this mutant forms heterotetramers with wild-type AQP2 and redirects this complex to the basolateral surface. The frame shift induces a change in the COOH terminus of AQP2, creating both a leucine- and a tyrosine-based motif, which cause the reversed sorting of AQP2. Our data reveal a novel cellular phenotype in dominant NDI and show that dominance of basolateral sorting motifs in a mutant subunit can be the molecular basis for disease.

Introduction

The renal action of the antidiuretic hormone arginine vasopressin (AVP) is essential in order to maintain osmo- and volume balance. With hypernatremia and hypovolemia, AVP is released from the pituitary and binds the vasopressin type-2 receptor at the basolateral side of collecting duct cells. Receptor occupation initiates a cAMP- and calcium-signaling cascade (Chou et al., 2000) that induces tethering of activated protein kinase A (PKA) to intracellular vesicles containing aquaporin-2 (AQP2; Klussmann et al., 1999). Subsequently, phosphorylation of minimally three monomers of an AQP2 tetramer, and possibly other proteins, results in a redistribution of AQP2 from intracellular vesicles to the apical plasma membrane, rendering this membrane water permeable (Nielsen et al., 1993; Katsura et al., 1997; Kamsteeg et al., 2000). Driven by the osmotic gradient, urinary water will then enter the cells via AQP2 and exit the cells to the interstitium via AQP3 and AQP4, which are constitutively present in the basolateral membrane.

In nephrogenic diabetes insipidus (NDI), this process of urine concentration is disturbed. Consequently, these humans suffer from polyuria and polydipsia. In congenital NDI, the autosomal form is caused by mutations in the *AQP2* gene (Deen et al., 1994). Expressed in *Xenopus* oocytes or mammalian cells, missense AQP2 mutants encoded in recessive NDI are misfolded and retained in the ER (Deen and Brown, 2001; Marr et al., 2002a). In dominant NDI, one missense and four (+1) frame-shift mutations of *AQP2* have been described (Mulders et al., 1998; Kuwahara et al., 2001; Marr et al., 2002b). The missense mutation encodes a mutant (AQP2-E258K) that is localized to the Golgi complex region in oocytes, whereas the mutants encoded by (+)1 frame shift mutations are localized to the endosomal/lysosomal compartments and/or the basolateral plasma membrane. The concomitant proteins are able to form hetero-oligomers with wild-type (wt) AQP2, in contrast to

Address correspondence to P.M.T. Deen, Dept. of Physiology, Nijmegen Center for Molecular Life Sciences, University Medical Center Nijmegen, Research Tower, 7th Floor, Geert 30, PO Box 9101, Nijmegen 6500 HB, Netherlands. Tel.: 31-24-3617347. Fax: 31-24-3616413. email: p.deen@ncmls.kun.nl

Key words: aquaporin; water channel; dominant disease; hetero-oligomerization; missorting

Abbreviations used in this paper: AP, adaptor protein complex; AQP2, aquaporin-2; AVP, arginine vasopressin; CLSM, confocal laser-scanning microscopy; NDI, nephrogenic diabetes insipidus; P_f, osmotic water permeability; PKA, protein kinase A; wt, wild type.

mutants in recessive NDI. The subsequent impaired routing of wt-AQP2 to the plasma membrane explains the dominant mode of inheritance of NDI (Kamsteeg et al., 1999; Kuwahara et al., 2001; Marr et al., 2002b). However, the molecular mechanism underlying the missorting of all mutants in dominant NDI is still unknown.

Here, we report a (−1) frame-shift mutation in the AQP2 gene causing dominant NDI. This mutant forms heterotetramers with wt-AQP2, and these complexes are missorted to the basolateral (instead of apical) plasma membrane. The frame shift results in a mutant AQP2 protein with a COOH terminus that is different from that of wt-AQP2 or the other mutants in dominant NDI. In this unique COOH terminus, we identified two basolateral sorting motifs that are responsible for the reversed sorting. These data provide the first molecular mechanism underlying the missorting of AQP2 in dominant NDI, and show for the first time that a dominant disease can result from a mutation that creates a basolateral sorting motif in a mutant subunit.

Results

Analysis of a family with dominant NDI

The proband P1 (Fig. 1) was referred to the clinic for a lifelong history of polyuria, polydipsia (8–10 l/d), and dilated bladder and ureters, as determined by ultrasound. Five of his six children and one grandchild (P2–7) also had polyuria and polydipsia. Clinical analyses of blood and urine revealed that all affected members of this family demonstrated mild hypernatremia (150 mmol/l) with concomitant low urine osmolarities (<200 mosM/kg H_2O) that did not increase after administration of the synthetic vasopressin analogue dDAVP. Therefore, NDI was diagnosed.

Subsequent segregation analysis within this family revealed that NDI cosegregated in a dominant fashion with markers located close to the AQP2 gene locus (Fig. 1). Sequence analysis of the complete *AQP2* gene from five patients (P1, 3–5, and 7) and four unaffected relatives (U1–4) revealed three mutations in the *AQP2* allele of the patients, but not in those of the healthy subjects. These mutations were a silent c501C>T mutation in exon 2, an insertion of an adenosine in exon 4 (c779-780insA), and a c836A>C mutation in the 3′ UTR. The c501C>T and c836A>C mutations are polymorphisms occurring with a frequency of 0.1 (n = 62) or 0.4 (n = 53; Marr et al., 2002b), respectively. However, the adenosine insertion causes a COOH-terminal frame shift that changes the last 12 amino acids of the AQP2 protein. In addition, with the c836A>C mutation in the same allele, which changes the new triplet TAA (stop codon) into TAC (Tyr), the C-tail of the encoded protein, which we denote AQP2-insA, is further extended with 14 amino acids (Fig. 2).

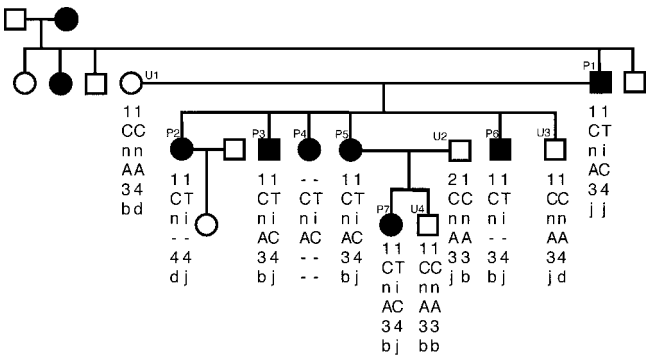

Figure 1. **Segregation of autosomal dominant NDI within the studied family.** Healthy (open symbols) and affected (filled symbols) individuals, and male (squares) and females (circles) are indicated. The 12q13 haplotype is represented using the marker order: centromere-AFM259vf9-*AQP2*-D12S131-AFMb007yg5-telomere. The lengths of simple sequence tags in nucleotides (AFM259vf9 [1:313; 2:315], D12S131 [3:156; 4:158], AFMb007yg5 [b:226; d:230; j:242]), the C or T polymorphism in exon 2, 779-780insA nucleotide insertion (i) or normal sequence (n), and the A or C polymorphism in the 3′ UTR of *AQP2* are indicated.

wt-AQP2

```
253  R  R  Q  S  V  E  L  H  S  P  Q  S  L  P  R  G  T  K  A  *
     CGGCGGCAGTCGGTGGAGCTGCACTCGCCGCAGAGCCTGCCACGGGGTACCAAGGCCTGA
```

AQP2-insA

```
253  R  R  Q  S  V  E  L  Q  L  A  A  E  P  A  T  G  Y  Q  G  L
     CGGCGGCAGTCGGTGGAGCTGCAACTCGCCGCAGAGCCTGCCACGGGGTACCAAGGCCTG

273  R  A  A  S  G  L  Y  G  P  D  G  R  L  *
     AGGGCCGCCAGCGGCCTCTACGGCCCCGACGGACGCTTGTGA
```

Figure 2. **COOH termini of wt-AQP2 and AQP2-insA.** The COOH-terminal amino acids (one-letter symbols) and corresponding nucleotide sequences of wild-type aquaporin-2 (wt-AQP2) and AQP2-insA are shown, starting at aa 253. The c779-780insA and c836A>C mutations, identified in the mutant AQP2 allele of the patient, are underlined and bold. An asterisk indicates a stop codon.

AQP2-insA is a functional water channel mainly localized in the plasma membrane

To determine the molecular cause of dominant NDI in this family, oocytes were injected with different amounts of cRNAs encoding wt-AQP2 or AQP2-insA. The osmotic water permeability (P_f) of AQP2-insA–expressing oocytes was significantly increased compared with noninjected oocytes, which indicated that AQP2-insA is a functional water channel. However, this P_f was slightly (but significantly) reduced compared with that of oocytes expressing wt-AQP2 (Fig. 3 A). To determine whether the reduced P_f of AQP2-insA was due to an overall lower expression level or reduced expression in the plasma membrane, total membranes and plasma membranes of the same oocytes were isolated and subjected to immunoblotting. In parallel, a serial dilution series of wt-AQP2 was immunoblotted to relatively quantify the obtained signals. With injections of ~0.3 ng, at which P_f values are in a linear range (Kamsteeg and Deen, 2000), wt-AQP2 and AQP2-insA were expressed at similar levels, but less AQP2-insA was detected in the plasma membrane fraction (Fig. 3 B). This indicated that the reduced P_f of oocytes expressing AQP2-insA is caused by a slight intracellular retention of AQP2-insA compared with wt-AQP2.

Fluorescence microscopy revealed that, in line with the similiar osmotic water permeabilities of AQP2-insA– and wt-AQP2–expressing oocytes, both AQP2-insA and wt-AQP2 were mainly expressed in the oocyte's plasma membrane

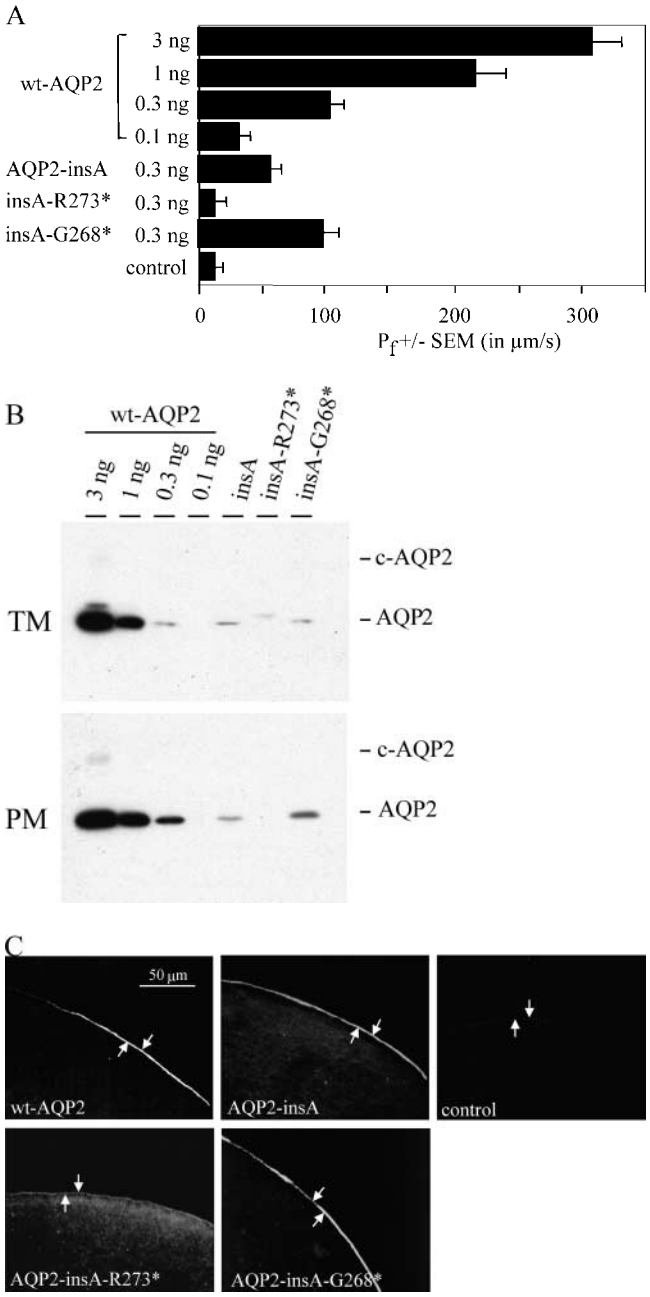

Figure 3. **Expression of AQP2-insA in oocytes.** (A) Water permeabilities. Oocytes were not injected (control), or injected with the indicated amounts of cRNA encoding wild-type AQP2 (wt-AQP2), AQP2-insA, AQP2-insA-R273* (insA-R273*), or AQP2-insA-G268* (insA-G268*). 2 d after injection, the mean water permeability ($P_f \pm$ SEM [in μm/s]; $n > 12$) was determined in a standard swelling assay. (B) AQP2 protein expression levels. Total membranes (TM) and plasma membranes (PM) of oocytes that were used for the P_f measurements were isolated, and equivalents of four oocytes were immunoblotted. To allow comparison of AQP2 protein amounts, the membranes were incubated with AQP2 antibodies that were completely preabsorbed with a synthetic peptide raised against the last 15 amino acids of wt-AQP2 (not depicted). Complex glycosylated and nonglycosylated AQP2 proteins are indicated by c-AQP2 and AQP2, respectively. (C) Subcellular localization of AQP2-insA proteins. 2 d after injection, noninjected oocytes (control) and oocytes injected with 0.3 ng cRNA encoding the indicated AQP2 proteins were fixed and embedded in paraffin. On 5-μm sections, AQP2 was visualized using rabbit AQP2 antibodies, followed by Alexa® 594–conjugated anti–rabbit IgGs. Arrows indicate the plasma membrane.

(Fig. 3 C). These data indicated that AQP2-insA is a functional water channel and that the dominant phenotype of AQP2-insA could not be demonstrated in oocytes.

AQP2-insA is redistributed from intracellular vesicles to the basolateral plasma membrane

Because renal collecting duct cells are epithelial cells, in contrast to oocytes, we speculated that the dominant phenotype might become clear when AQP2-insA would be expressed in the epithelial MDCK (type I) cells, which are derived from renal collecting ducts. Heterologously expressed in these cells, wt-AQP2 is redistributed from vesicles to the apical membrane on stimulation with AVP or forskolin (Deen et al., 1997). Therefore, MDCK cell lines stably expressing

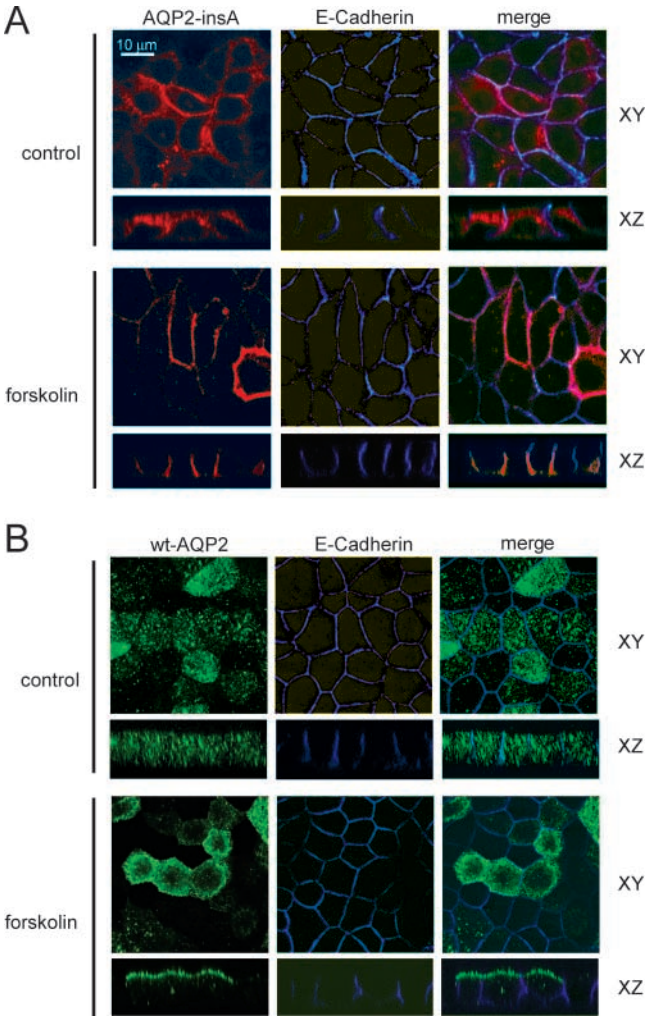

Figure 4. **Localization of AQP2-insA in MDCK cells.** MDCK cells expressing AQP2-insA (A) or wt-AQP2 (B) were grown to confluence, incubated without (control) or with forskolin, fixed, and immunostained using guinea pig AQP2-insA antibodies followed by an incubation with Alexa® 594–conjugated anti–guinea pig IgGs (red) or rabbit AQP2 antibodies, followed by Alexa® 488–conjugated anti–rabbit IgGs (green). The basolateral marker protein E-cadherin was visualized using specific rat antibodies followed by Cy5-conjugated anti–rat IgGs. Horizontal (XY) and vertical (XZ) images for AQP2-insA, wt-AQP2, and E-cadherin were obtained with a confocal laser-scanning microscope and merged (merge).

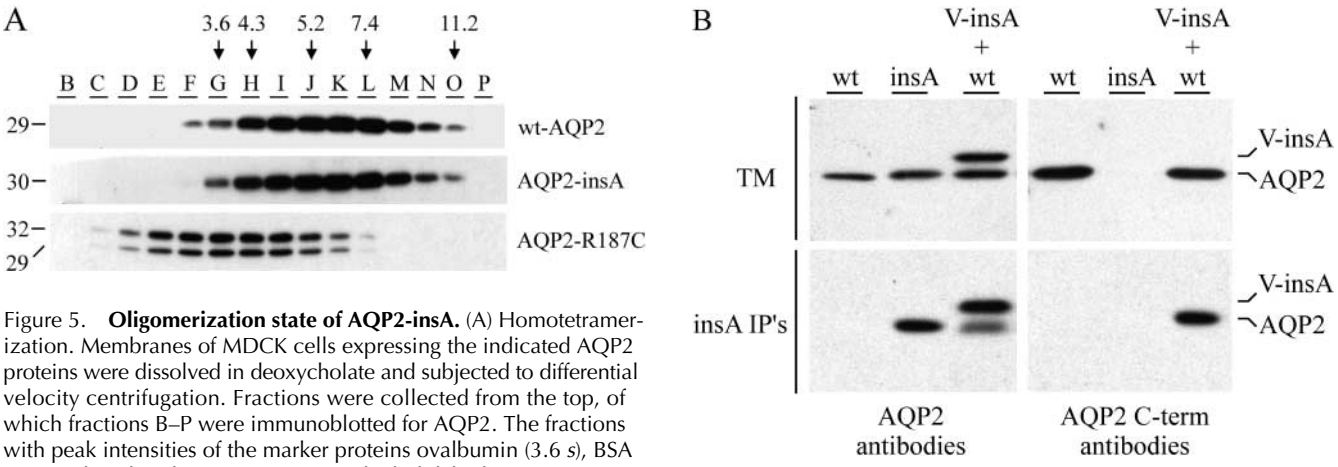

Figure 5. **Oligomerization state of AQP2-insA.** (A) Homotetramerization. Membranes of MDCK cells expressing the indicated AQP2 proteins were dissolved in deoxycholate and subjected to differential velocity centrifugation. Fractions were collected from the top, of which fractions B–P were immunoblotted for AQP2. The fractions with peak intensities of the marker proteins ovalbumin (3.6 *s*), BSA (4.3 *s*), phosphorylase B (5.2 *s*), yeast alcohol dehydrogenase (7.4 *s*), and catalase (11.2 *s*) are indicated by arrows and by their sedimentation values. The molecular masses (in kD) of the respective AQP2 proteins are indicated on the left. (B) Heteroligomerization of AQP2-insA with wt-AQP2. Membranes of MDCK cells expressing wt-AQP2 (wt), AQP2-insA (insA), or VSV-G-tagged AQP2-insA together with wt-AQP2 (V-insA + wt) were solubilized in deoxycholate and centrifuged to remove nonsolubilized material. The supernatants were directly subjected to immunoblotting (TM, total membranes) or subjected to immunoprecipitation with affinity-purified AQP2-insA antibodies (insA IPs), followed by immunoblotting. Transferred AQP2 proteins were detected with rabbit AQP2 antibodies that recognize wt-AQP2 and AQP2-insA, or with affinity-purified rabbit AQP2 COOH-terminal antibodies (AQP2 C-term antibodies) that do not recognize AQP2-insA. Specific bands for VSV-G–tagged AQP2-insA (V-insA) and untagged AQP2 proteins (AQP2) are indicated on the right.

AQP2-insA were obtained and analyzed. Immunocytochemistry and confocal laser-scanning microscopy (CLSM) analysis revealed that without stimulation, AQP2-insA was mainly localized in intracellular vesicles, which were differently distributed than those containing wt-AQP2 (Fig. 4, A and B; control). In addition, forskolin stimulation resulted in redistribution of AQP2-insA to the basolateral membrane, at which it colocalized with the basolateral marker protein E-cadherin (Fig. 4 A, forskolin). In contrast, wt-AQP2 was redistributed from intracellular vesicles to the apical membrane on stimulation (Fig. 4 B, forskolin).

AQP2-insA forms hetero-oligomers with wt-AQP2

The missorting of hetero-oligomers of wt-AQP2 and its mutants was shown to provide an explanation for dominant NDI. To study if AQP2-insA would cause NDI through a similar mechanism, membranes of MDCK cells expressing wt-AQP2, AQP2-insA, or AQP2-R187C (a mutant in recessive NDI) were solubilized and subjected to differential velocity centrifugation. Immunoblot analysis of gradient fractions and comparison of their signal peak fraction with that of marker proteins revealed that AQP2-insA and wt-AQP2 have sedimentation coefficients in between 4.3 and 7.4 (Fig. 5 A). These coefficients conform to expression of AQP1 and AQP4 as homotetramers because the homotetrameric AQP1 and AQP4 are ~5.7 *s* and 5.2–6.8 *s*, respectively (Smith and Agre, 1991; Neely et al., 1999). As shown before in oocytes (Kamsteeg et al., 1999), AQP2-R187C, which is expressed as nonglycosylated (29 kD) and high-mannose glycosylated (32 kD) forms, has a sedimentation coefficient of ~4.3 (Fig. 5 A), which indicated that AQP2-R187C is also expressed as a monomer in MDCK cells.

To determine whether wt-AQP2 and AQP2-insA heteroligomerize, wt-AQP2–expressing cells were supertransfected with an expression construct encoding VSV-G–tagged AQP2-insA (V-AQP2-insA). This tag, which does not interfere with the basolateral localization of AQP2-insA, allows discrimination of AQP2-insA from wt-AQP2 on immunoblot because it retains its migration on SDS-PAGE. Representative clonal cell lines expressing similar levels of both wt-AQP2 and V-AQP2-insA (Fig. 5 B, top left, third lane), or wt-AQP2 and AQP2-insA alone were grown to confluence. Total membranes were isolated, solubilized, and directly immunoblotted or subjected to immunoprecipitation using AQP2-insA–specific antibodies. Detection of transferred proteins from total membranes with AQP2 antibodies (which recognize wt-AQP2 and AQP2-insA) and AQP2 COOH-terminal antibodies (which recognize only wt-AQP2) confirmed the expression of wt-AQP2 or AQP2-insA in the single transfectants and of wt-AQP2 and V-AQP2-insA in coexpressing cells (Fig. 5 B). Analysis of the immunoprecipitates (bottom) revealed that wt-AQP2 coprecipitated with V-AQP2-insA, which indicated that AQP2-insA and wt-AQP2 formed hetero-oligomers. Similar results were obtained when these proteins were (co)expressed in oocytes (unpublished data).

AQP2-insA directs wt-AQP2 to the basolateral membrane

When expressed alone, wt-AQP2 is sorted to the apical plasma membrane and AQP2-insA to the basolateral plasma membrane of MDCK cells. Because their coexpression in MDCK cells results in the formation of hetero-oligomers, we analyzed where these complexes were sorted to. Immunocytochemistry and CLSM analysis showed that wt-AQP2 and V-AQP2-insA colocalized to a large extent in intracellular vesicles (Fig. 6 A, control). On stimulation with forskolin, wt-AQP2 was translocated to the basolateral membrane together with V-AQP2-insA (Fig. 6 A, forskolin). As a negative control, wt-AQP2–expressing MDCK cells were super-

transfected with an expression construct encoding AQP2-R187C, which was NH_2-terminally tagged with GFP (G-AQP2-R187C; for consistency, wt-AQP2 is given in green, and G-AQP2-R187C is shown in red). In these cells, wt-AQP2 showed a vesicular expression pattern and shifted to the apical plasma membrane upon forskolin stimulation (Fig. 6 B). However, G-AQP2-R187C showed a dispersed staining that was clearly different from that of wt-AQP2 and did not change upon forskolin treatment (Fig. 6 B). These results revealed that assembly of wt-AQP2/AQP2-insA complexes resulted in the sorting of wt-AQP2 to the basolateral membrane, which provides an explanation for dominant NDI in this particular family.

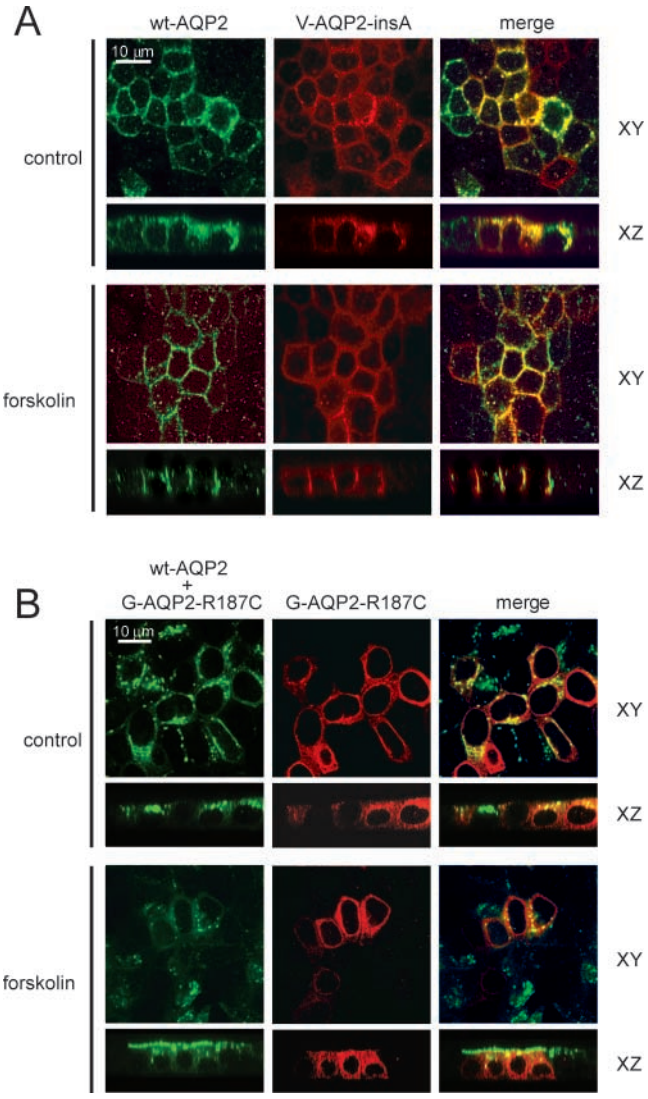

Figure 6. **Colocalization and regulation of AQP2-insA and wt-AQP2 in MDCK cells.** (A) MDCK cells coexpressing wt-AQP2 and VSV-G–tagged AQP2-insA were incubated without (control) or with forskolin, fixed, and incubated with rabbit AQP2 COOH-terminal antibodies and guinea pig AQP2-insA antibodies, followed by Alexa® 488–conjugated anti–rabbit IgGs (green) and Alexa® 594–conjugated anti–guinea pig IgGs (red). Horizontal (XY) and vertical (XZ) images for wt-AQP2 and VSV-G–tagged AQP2-insA (V-AQP2-insA) were obtained with a confocal laser-scanning microscope and merged (merge). (B) MDCK cells heterologously expressing wt-AQP2 were supertransfected with a plasmid encoding GFP-tagged AQP2-R187C, and GFP-positive cells were selected using FACS® analysis. These pooled cells were grown to confluence on filter supports, treated as under A, and incubated with rabbit AQP2 COOH-terminal antibodies that recognize both wt-AQP2 and AQP2-R187C (wt-AQP2 + G-AQP2-R187C), followed by Alexa® 594–conjugated anti–rabbit IgGs (shown in green pseudocolor). The GFP signal of AQP2-R187C (G-AQP2-R187C) is given the red pseudocolor. Horizontal (XY) and vertical (XZ) images for were obtained with a confocal laser-scanning microscope and merged (merge).

AQP2-insA contains two basolateral sorting signals

The basolateral sorting of AQP2-insA could be caused by the loss of apical sorting signals contained in the COOH terminus of wt-AQP2 or by the presence of basolateral sorting signals in the COOH-terminal tail of AQP2-insA. To analyze whether lacking the COOH-terminal tail of wt-AQP2 could be the cause of the basolateral sorting of AQP2-insA, MDCK clones stably expressing AQP2-S261* were made. The translation of this mutant is stopped, whereas in AQP2-insA the reading frame changes. Forskolin induced a translocation of AQP2-S261* from vesicles to the apical membrane (Fig. 7 A, w-S261*), although this was less efficient as found for wt-AQP2. However, this indicated that the basolateral sorting of AQP2-insA was not caused by a deletion of an apical determinant in wt-AQP2, but by basolateral sorting information in the COOH terminus of AQP2-insA.

To identify such information in AQP2-insA, constructs encoding AQP2-insA with stop codons after D282, Y279, R273, G268, or E264 were made and stably transfected to MDCK cells. All these truncation mutants were still sorted to the basolateral plasma membrane, with varying dependence on forskolin stimulation (Fig. 7 A). Therefore, the COOH-terminal four amino acids in AQP2-insA-E264* should contain a basolateral sorting signal, because this stretch of amino acids was the only difference with AQP2-S261*. Because leucine-based motifs in cytoplasmic tails can mediate sorting to the basolateral membrane (Heilker et al., 1999; Wehrle-Haller and Imhof, 2001), the involvement of L261 in the basolateral sorting of AQP2-insA was analyzed. Indeed, substitution of alanine for L261 in AQP2-insA-G268* (AQP2-insA-L261A-G268*) resulted in localization in the apical plasma membrane. To confirm the role of L261 in the basolateral sorting of AQP2-insA, the L261A substitution was introduced into the full-length AQP2-insA, AQP2-insA-L261A. However, this mutant is translocated to the basolateral surface, which indicated that another basolateral sorting determinant must be present downstream of L261. Tyrosine-based motifs with the consensus YXXØ (X is any amino acid; Ø is an amino acid with a bulky hydrophobic side chain) are also known basolateral sorting signals (Hunziker et al., 1991; Folsch et al., 1999), and the Y_{269}QGL sequence in AQP2-insA fits to this consensus. Because the tyrosine is critical in this element, the Y269A substitution was introduced into AQP2-insA and AQP2-insA-L261A. CLSM analysis revealed that AQP2-insA-Y269A was sorted to the basolateral plasma membrane, whereas AQP2-insA-L261A-Y269A was sorted to the apical plasma membrane (Fig. 7). Thus, our data show that two motifs are involved in the basolateral sorting of AQP2-insA.

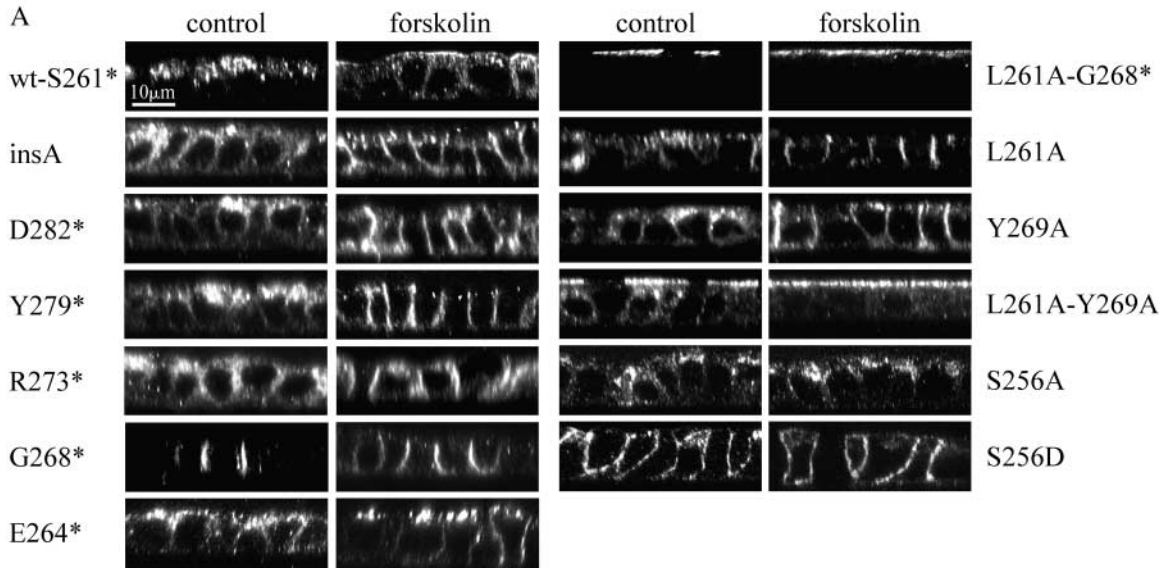

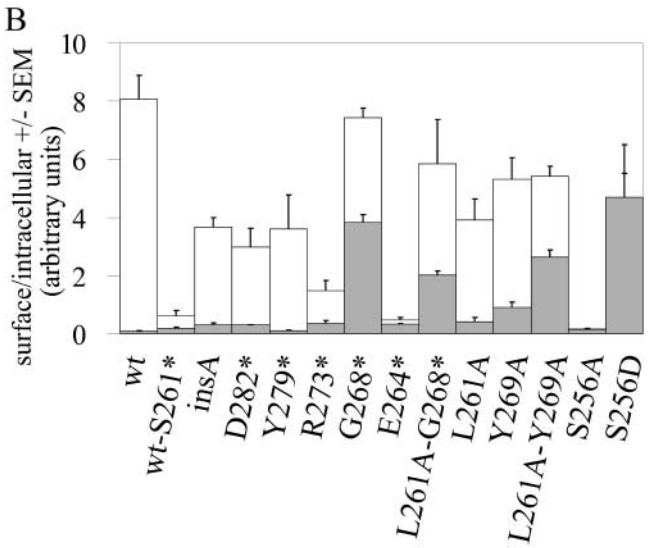

Figure 7. **Subcellular localization of AQP2-insA mutants in MDCK cells.** (A) MDCK cells stably expressing AQP2-S261* (wt-S261*) or AQP2-insA mutants (indicated by insA or introduced mutations; asterisks indicate stop codons) were incubated without (control) or with forskolin, fixed, and immunostained for AQP2 proteins using rabbit AQP2 and Alexa® 594–conjugated anti–rabbit antibodies. XZ images were made with a confocal laser-scanning microscope. (B) Mean values of integrated OD of surface or intracellular staining of AQP2 proteins were obtained from confocal laser-scanning microscope images. The ratio between surface and intracellular expression (ratio surface/intracellular ± SEM; $n > 8$) is determined from these values. Gray bars indicate this ratio from untreated cells, total bars indicate this ratio after forskolin stimulation.

Phosphorylation of AQP2-insA at S256 induces its redistribution to the basolateral membrane

Both wt-AQP2 and AQP2-insA redistributed from intracellular vesicles to the plasma membrane with forskolin (Fig. 4 and Fig. 7 A). For wt-AQP2, this translocation depends on phosphorylation of S256 in its COOH terminus by PKA (Katsura et al., 1997; van Balkom et al., 2002). Phosphorylation-state mutants of AQP2 perfectly mimic this effect (i.e., AQP2-S256A is localized in intracellular vesicles, whereas AQP2-S256D is present in the apical plasma membrane, both with or without forskolin; van Balkom et al., 2002). Because AQP2-insA still contains this PKA consensus site, we tested its role in the shuttling of AQP2-insA by introducing the S256A and S256D mutations. Indeed, CLSM analysis revealed that AQP2-S256A-insA was retained in intracellular vesicles, whereas AQP2-S256D-insA was localized in the basolateral membrane, independent of forskolin treatment (Fig. 7 A). These data indicated that the translocation of AQP2-insA from intracellular vesicles to the basolateral membrane also relies on the phosphorylation of S256 in its COOH terminus.

The YXXØ motif in AQP2-insA causes a decrease in surface expression

The obvious differences in plasma membrane expression levels of the AQP2-insA mutants with or without forskolin (Fig. 7 A) indicated that S256 phosphorylation is not the only determinant of their subcellular localization. To identify other elements involved in this behavior, we performed computer-assisted image analysis of the cell surface/intracellular expression pattern, in which colocalization with E-cadherin was used to identify the basolateral plasma membrane (unpublished data). This analysis revealed three different phenotypes (Fig. 7 B). First, similar to wt-AQP2 and AQP2-insA, several mutants show a predominant intracellular staining without forskolin and a marked translocation to the plasma membrane after forskolin stimulation (AQP2-insA-D282*, -Y279*, -L261A, and -Y269A). Second, some mutants are already mainly present in the cell surface with-

out forskolin stimulation (AQP2-insA-G268*, -L261A-G268*, and -L261A-Y269A). Third, three mutants show a marked decrease in their plasma membrane expression, even after forskolin stimulation (wt-AQP2-S261*, and AQP2-insA-E264* and -R273*). In the latter group, wt-AQP2-S261* and AQP2-insA-E264* are probably inefficiently sorted due to their short COOH termini. Strikingly, however, all AQP2-insA mutants that contain the YXXØ motif are vesicularly localized when untreated, whereas AQP2-insA-R273*, which has the YXXØ motif at its extreme COOH terminus, even remains intracellularly localized when stimulated with forskolin. In contrast, those that lack this motif are already partially localized in the plasma membrane in untreated cells.

Involvement of the YXXØ motif in vesicular localization is also supported from the oocyte analyses. At similar total expression levels, AQP2-insA was expressed at lower levels in the plasma membrane than wt-AQP2 (Fig. 3 B). Therefore, AQP2-insA-R273* and AQP2-insA-G268* were also expressed in oocytes. Compared with wt-AQP2 or AQP2-insA, oocytes expressing AQP2-insA-R273* showed a strongly reduced P_f, whereas the P_f of oocytes expressing AQP2-insA-G268* was not different from those injected with the corresponding amount of wt-AQP2 cRNA (Fig. 3 A). Immunoblot analysis of total and plasma membrane fractions of these oocytes revealed that the total expression levels of wt-AQP2 and the three mutants were similar (Fig. 3 B, TM; 0.3-ng injections). The plasma membrane expression of AQP2-insA-G268* was similar to that of wt-AQP2, whereas AQP2-R273* was not detected in the plasma membrane fraction at all (Fig. 3 B), even at higher expression levels (unpublished data). The reason for the slower migration of AQP2-insA-R273* in SDS-PAGE is unclear, but consistent in oocytes (Fig. 3 B) and MDCK cells (unpublished data). Consistent with the functional and biochemical data, immunocytochemistry of these oocytes revealed that AQP2-insA-R273* was predominantly localized in intracellular vesicles, whereas AQP2-insA-G268* was, as wt-AQP2, only detected in the plasma membrane (Fig. 3 C). Altogether, these data reveal that the YXXØ motif in AQP2-insA causes a decreased plasma membrane localization of this mutant.

Discussion

AQP2-insA is missorted to the basolateral plasma membrane

Here, we report a new mutant in dominant NDI, AQP2-insA, which was mainly expressed in the plasma membrane of oocytes and sorted to the basolateral (instead of the apical) plasma membrane of MDCK cells (Fig. 3 and Fig. 4 A). This is similar to the localization of other basolateral proteins, such as AQP3/4, I'm not dead yet (Indy), and the inwardly rectifying potassium channel Kir2.1, when expressed in oocytes (Ishibashi et al., 1994; Jung et al., 1994; Knauf et al., 2002; Wild and Paysan, 2002). Five other AQP2 gene mutations in dominant NDI have been reported that encode AQP2-E258K and four nucleotide deletion mutants (Mulders et al., 1998; Kuwahara et al., 2001; Marr et al., 2002b). In contrast to AQP2-insA, all five mutants are largely impaired in their routing to the plasma membrane in oocytes. AQP2-E258K is missorted to the Golgi complex region of oocytes, whereas the aberrant localization of the four deletion mutants has not yet been determined in these cells. Previously, we described that one of the deletion mutants, AQP2–727delG, accumulated in late endosomes/lysosomes and, to some extent, in the basolateral plasma membrane of MDCK cells (Marr et al., 2002b). Because the other deletion mutants in dominant NDI (721delG, del763–772, and del812–818) have a similar extended COOH terminus as AQP2–727delG, due to a (+1) reading frame shift, and are also retained in oocytes, their complete localization to the basolateral plasma membrane of MDCK cells (Asai et al., 2003) was rather surprising.

Phosphorylation of AQP2-insA is required for its basolateral plasma membrane insertion

In wt-AQP2, phosphorylation of S256 is essential for its translocation from vesicles to the apical plasma membrane (van Balkom et al., 2002). The localization of AQP2-insA-S256A and AQP2-insA-S256D reveals that phosphorylation of S256 is also fundamental to the forskolin-induced translocation of AQP2-insA, albeit here from vesicles to the basolateral plasma membrane. This corroborates with the current opinion that trafficking to both plasma membranes of MDCK cells is regulated by (de)phosphorylation events (Brewer and Roth, 1995). Due to the high intracellular cAMP levels (Hoffman et al., 1994; Xu et al., 1996), AQP2 is completely phosphorylated in oocytes, and therefore predominantly present in the plasma membrane (Kamsteeg et al., 2000). Therefore, it is not surprising that AQP2-insA is also located in the plasma membrane of oocytes.

A leucine- and a tyrosine-based motif cause basolateral sorting of AQP2-insA

Routing experiments have shown that dileucine motifs (in which one may be replaced by isoleucine, valine, or methionine) and tyrosine-based motifs in cytoplasmic termini often target proteins to the basolateral plasma membrane (Sandoval and Bakke, 1994; Heilker et al., 1999). Although both a dileucine- and a tyrosine-based motif were needed for basolateral expression of the interleukin-6 receptor gp80 (McClure and Robinson, 1996), most proteins contain one dileucine- or tyrosine-based element, which is sufficient for their basolateral sorting. To identify the segments conferring the basolateral sorting of the wt-AQP2/AQP2-insA complexes, several mutants were analyzed for their subcellular localization before and after forskolin stimulation. This revealed that AQP2-insA was targeted to the apical membrane when L261 and Y269 were both absent, but not independently (Fig. 7). These data clearly revealed that, like AQP4 (Madrid et al., 2001), AQP2-insA contains two independently acting basolateral sorting motifs. The Y_{269}QGL sequence meets the criteria for a canonical tyrosine-based sorting motif. These tyrosine-based motifs can be recognized by adaptor protein complexes (APs), which direct sorting. Six different APs (1A, 1B, 2, 3A, 3B, and 4) have been identified with different functions and or tissue distribution (Robinson and Bonifacino, 2001). AP1B and AP4 are thought to direct baso-

lateral sorting (Folsch et al., 1999; Simmen et al., 2002) and therefore, could also be involved in basolateral sorting of AQP2-insA. L261 in AQP2-insA is not part of a typical dileucine motif because it is not flanked by an isoleucine, valine, or methionine. However, it has recently been reported that a single leucine is sufficient for basolateral sorting of the stem cell factor (Wehrle-Haller and Imhof, 2001). Therefore, L261 in AQP2-insA seems to be the second monoleucine identified that is able to target a protein to the basolateral membrane. To date, no interaction partners for monoleucine motifs have been identified. The basolateral missorting of AQP2-insA by two COOH-terminal motifs comprise the first molecular mechanism underlying the missorting of AQP2 in dominant NDI.

The tyrosine-based motif of AQP2-insA also decreases surface expression

The tyrosine-based motif in AQP2-insA seems to decrease its surface expression because AQP2-insA mutants that still contain this motif showed a clear intracellular localization in both oocytes and MDCK cells (Fig. 3 and Fig. 7). In contrast, those that lack this motif are readily present in the oocyte plasma membrane, and partially localized to the plasma membrane of untreated MDCK cells. Besides directing basolateral sorting, tyrosine-based motifs are also involved in endocytosis, although with somewhat different sequence requirements (Hunziker et al., 1991; Prill et al., 1993). Therefore, the tyrosine-based motif of AQP2-insA probably also acts as an internalization motif. Typically, AP2 is involved in rapid endocytosis of proteins with tyrosine-based motifs (Nesterov et al., 1999). Data from Ohno et al. (1996) show that the interaction of a tyrosine-based sorting motif with AP2 is strongest when located at the COOH-terminal end. Similarly, AQP2-insA-R273*, which also has its tyrosine-based motif at its extreme COOH terminus, is predominantly intracellularly localized in oocytes and remains mainly localized in vesicles of MDCK cells after forskolin treatment.

A novel cellular phenotype in dominant NDI: two independent basolateral sorting motifs in AQP2-insA subunits overrule apical targeting signals in wt-AQP2 subunits

In MDCK cells, hetero-oligomers of wt-AQP2 and AQP2-insA are missorted to the basolateral plasma membrane due to basolateral sorting motifs in the mutant (Fig. 6 A). Extrapolated to the kidney, the missorting of wt-AQP2 to the basolateral membrane upon interaction with AQP2-insA will result in decreased renal water reabsorption through the apical plasma membrane, and therefore provides a cell-biological explanation for NDI in this particular family.

Apical sorting of proteins is mediated through formation of glycolipid- and cholesterol-containing membrane subdomains (i.e., rafts) in the TGN and through N-linked glycans, but can also occur independently from these processes (Scheiffele et al., 1995; Simons and Ikonen, 1997). No apical sorting information has yet been identified in AQP2. Basolateral sorting signals are thought to be dominant over apical sorting information because fusion of basolateral sorting motifs to apical proteins (Casanova et al., 1991), or even single amino acid substitutions in an apical protein (Brewer and Roth, 1991), can redirect these proteins to the basolateral surface. The seemingly complete basolateral sorting of wt-AQP2/AQP2-insA heterotetramers underscores this phenomenon.

At present, only a few other diseases have been described in which the introduction or deletion of a sorting signal is the molecular basis of a disease. A mutant low density lipoprotein receptor, which was found in familial hypercholesterolemia, has a defect in one of its tyrosine-based motifs. This mutant is missorted to the apical (instead of basolateral) plasma membrane of MDCK cells and to the bile canalicular (apical) surface of cultured hepatocytes and mouse liver in vivo (Koivisto et al., 2001). In addition, early stop mutants of the cystic fibrosis transmembrane conductance regulator, which lacked a PDZ motif and were not able to bind the apical membrane protein EBP50, accumulated at the basolateral membrane (Moyer et al., 1999). However, both proteins are thought to function as monomers because cystic fibrosis is a recessive trait and familial hypercholesterolemia has a dominant form of inheritance probably caused by haplotype insufficiency. As such, our data reveal a novel cellular phenotype in dominant NDI and show for the first time that dominance of basolateral targeting motifs in mutant subunits over apical targeting signals in wt subunits in a heterotetramer can be the molecular basis of a dominant disease. Because many ion channels in diseases are expressed as multimers (e.g., ROMK1, KIR6.2; Glowatzki et al., 1995; Tinker et al., 1996; Verkarre et al., 1998), missorting of a channel complex due to the introduction of sorting motifs in a mutant monomer might also be fundamental to other dominant diseases.

Materials and methods

Patients: clinical analysis, haplotype analysis, and mutation detection

Clinical analysis of blood and urine osmolarities was done by standard procedures. Haplotype analysis was performed for three dinucleotide repeats (*AFM259vf9*, *D12S131*, and *AFMb007yg5*) flanking the AQP2 gene (LeBlanc Straceski et al., 1994), and for a putative benign mutation of the AQP2 gene (c.836A>C, 3′ UTR). For interpretation of the haplotype data, we assumed no recombination within an ~1.5-megabase region spanned by *AFM259vf9* and *AFMb007yg5*. The provided haplotype data support the consistency of the stated biologic parentage within the pedigree. Identification of the AQP2 gene mutations described in this paper was essentially done as described earlier (Bichet et al., 1993).

DNA constructs

General. Mutations were introduced by in vitro mutagenesis (altered sites [Promega] or QuikChange® [Stratagene]) or PCR using *Pfu* DNA polymerase (Stratagene). Clones with the desired mutations were identified by the introduced restriction sites (underlined), after which the proper sequence of the inserts was verified by DNA sequence analysis.

Oocyte expression constructs. To introduce the AQP2–779–780insA mutation into the AQP2 cDNA, the primer 5′-GGTGGAGCTGCA**G**CTGGC-CGCAGAGCCT-3′ was with pAlter-AQP2 (Mulders et al., 1998). Instead of an adenosine, a guanidine (bold) was inserted to silently introduce a PvuII site. A 200-bp NarI and blunted HindIII fragment, containing the mutation, was isolated and cloned into the NarI and EcoRV sites of pBS-AQP2 (Deen et al., 1994), generating pBS-insA. Next, a 282-bp BamHI/KpnI fragment from this clone was subcloned into the corresponding sites of pT_7T_S-wt-AQP2 to create pT_7T_S-insA-1. Because the AQP2–779–780insA mutation extends the protein by 14 amino acids, the 3′ UTR of the human AQP2 gene needed to be cloned in. Therefore, a 426-bp PCR fragment was generated from human genomic DNA using the forward primer 511F

(5′-CACCGGCTGCTCTATGAATCCT-3′) and the reverse primer (5′-ACTAGTCAGACTGCGGGAGAGGAGGGACG-3′), and was subcloned into the EcoRV site of pBSIIKS+. Subsequently, the c836A>C mutation, which was also found in the mutant AQP2 allele, was introduced with the forward primer 5′-CCTGAGGGCCGCTAGCGGCCTCTACGGCCCCGACGG-3′. From this clone, pBS-UTR, an 80-bp KpnI/blunted ApaI fragment was isolated and cloned into the KpnI/blunted SpeI sites of the oocyte's expression vector pT_7T_S-insA to generate pT_7T_S-insA.

The insA-R273* and insA-G268* mutations were introduced by PCR on pBS-insA using the 533F forward primer 5′-CCCCTGCTCTCTCCATAGGC-3′ and the reverse primers 5′-GTACCAAGGCCTCTAGACCGCCAGCCCGT-3′ and 5′-AGAGCCTGCCACCTAGGACCAAGGCCTGA-3′, respectively. The PCR fragments were digested with BamHI and ligated into the EcoRV/BamHI sites of pBS-AQP2. From these clones, 320-bp BamHI/blunted HindIII fragments were isolated and cloned into the BamHI/blunted SpeI sites of pT7Ts-AQP2, resulting in pTsT7-insA-R273* and pTsT7-insA-G268*.

Mammalian expression constructs

The AQP2-S261*–encoding mutation was obtained with the reverse primer 5′-GAGCTGCACTAGTCGCAGAGCCT-3′. Subsequently, a 282-bp BamHI/KpnI AQP2 fragment of pTsT7-AQP2 was exchanged for its mutant fragment. pCB6-AQP2-S261* was made by ligation of the 870-bp BglII/SpeI fragment from pTsT7-AQP2-S261* into BglII/XbaI-restricted pCB6. To generate pCB6-AQP2-R187C, a BglII/SpeI fragment from pTsT7-AQP2-R187C (Deen et al., 1994) was subcloned into the BglII/XbaI sites of pCB6. To facilitate cloning of other AQP2 cDNAs into pCB6, the BamHI site of pCB6 was removed. To clone AQP2-insA into pCB6, a two-step cloning procedure was performed. First, a 120-bp KpnI fragment from pBS-UTR was cloned into the KpnI site of pBS-insA. Second, a 950-bp blunted EcoRI/XbaI fragment was cloned into the blunted SacI and XbaI sites of pCB6ΔBamHI. pCB6-insA-R273* and pCB6-insA-G268* were made by ligation of 920-bp NotI/HincII fragments of pBS-insA-R273* and pBS-insA-G268*, respectively, into NotI/blunted XbaI pCB6. The pCB6 constructs encoding insA-L261A, insA-Y269A, insA-E264*, insA-Y279*, and insA-D282* were obtained with the forward primers 5′-GGAGCTGCAGGCCGCCGCGGAGCCTGCCAC-3′, 5′-CGCAGAGCCTGCCACGGGGGCCCAAGGCCTGAGGGCCGC-3′, 5′-GCTCGCCGCATAAGCTTCCACGGGGTACC-3′, 5′-CCTGAGGGCCGCTAGCGGCCTCTAAGGCCCCGACGG-3′, and 5′-GCGGCCTCTACGGCCCCTAGGGACGCTTGTG-3′, respectively, and a pCB6ΔBamHI template. For pCB6-insA-L261A-G268* and pCB6-insA-L261A-Y269A, the insA-L261A primers were used on pCB6-insA-G268* and pCB6-insA-Y269A templates, respectively. Subsequently, the BamHI/XbaI fragment of pCB6ΔBamHI was exchanged for that of those seven mutants.

To generate a construct encoding VSV-G–tagged AQP2-insA, a 300-bp BamHI/HincII fragment from pBS-insA was isolated and ligated into the BamHI/blunted SalI sites of pBS-wt-VSV-G-AQP2 (Kamsteeg et al., 1999). Subsequently, a blunted NotI/HindIII fragment from this clone was subcloned into the blunted BglII/HindIII sites of pCB6. To generate pEGFP-AQP2-R187C, a 1,083-bp blunted NspI/SalI fragment of pTsT7-AQP2-R187C (Deen et al., 1994) was isolated and cloned into the HindIII blunted/SalI sites of pEGFP-C1 (CLONTECH Laboratories, Inc.).

AQP2 antibodies

Affinity-purified antibodies specific for the COOH terminus of AQP2 (AQP2 COOH-terminal antibodies) and those raised against aa 175–269 of human AQP2 (AQP2 antibodies) have been described previously (Deen et al., 1994; Mulders et al., 1998). To generate AQP2-insA antibodies, a 275-bp PvuII fragment, encoding the C-tail of AQP2-insA, was isolated from pBS-insA and ligated into the SmaI site of pGEX3X (Amersham Biosciences). The isolation of the soluble GST fusion protein and generation of affinity-purified AQP2-insA antibodies was done as described previously (Marr et al., 2002b).

Expression in oocytes

Transcription of pT_7T_s constructs, and isolation, injection, and P_f measurements of *Xenopus* oocytes were done as described previously (Mulders et al., 1998). Total and plasma membranes were isolated as described previously (Kamsteeg and Deen, 2001). Immunocytochemistry was done as described elsewhere (Mulders et al., 1998) using 1:50 diluted affinity-purified AQP2 antibodies.

Membrane isolation from MDCK cells

To isolate total membranes, MDCK cells were grown to confluence in a 10-cm dish, scraped in PBS, and spun down at 200 *g* for 5 min at 4°C. The cells were homogenized in 2.5 ml HbA (20 mM Tris, pH 7.4, 5 mM $MgCl_2$, 5 mM NaH_2PO_4, 1 mM EDTA, 80 mM sucrose, and protease inhibitors) using a mortar and pestle. Unbroken cells and nuclei were removed by centrifugation at 1,000 *g* for 10 min at 4°C. Membranes were spun down at 100,000 *g* for 1 h at 4°C.

Differential velocity centrifugation and immunoprecipitation

Membranes of MDCK cells from a 10-cm dish or membranes of 60 oocytes were solubilized in 300 μl 4% sodium-deoxycholate. Gradient centrifugation and immunoprecipitation of protein complexes from these solubilized membranes was performed as described previously (Kamsteeg et al., 1999). Specific immunoprecipitation of AQP2-insA was performed similarly, using 30-μl equivalents of protein G–agarose beads (Amersham Biosciences), preincubated with 10 μl affinity-purified guinea pig AQP2-insA antibody.

Immunoblotting

PAGE, blotting, and blocking of the membranes was performed as described previously (Kamsteeg et al., 1999). Membranes were incubated overnight with a 1:3,000 dilution of affinity-purified rabbit AQP2 or AQP2-COOH-terminal antibodies. In experiments where the expression levels between wt-AQP2 and AQP2-insA were compared, the AQP2 antibodies were completely preabsorbed with a synthetic peptide raised against the last 15 amino acids of AQP2. Preabsorption was complete when the wt/wt ratio of peptide versus antibody was 3. All primary antibodies were diluted in TBS-T (20 μM Tris, 140 NaCl, and 0.1% Tween 20, pH 7.6) supplemented with 1% nonfat-dried milk. Blots were incubated for 1 h with 1:5,000-diluted goat anti–rabbit IgGs or 1:2,000 goat anti–mouse IgGs (Sigma-Aldrich) as secondary antibodies coupled to HRP. Proteins were visualized using ECL (Pierce Chemical Co.).

Culture and immunocytochemistry on MDCK cells

MDCK cells were grown and transfected, and immunocytochemistry and collection of images were performed as described previously (Deen et al., 2002). Three clonal cell lines per mutant were analyzed to exclude the possibility that clonal differences might cause the observed phenotypes. As primary antibodies, a 1:100 dilution of affinity-purified rabbit AQP2 or AQP2-COOH-terminal antibodies, a 1:10 dilution of affinity-purified guinea pig AQP2-insA, or a 1:500 dilution of affinity-purified rat E-cadherin antibodies (Sigma-Aldrich) were used. As secondary antibodies, 1:100 dilutions of affinity-purified goat anti–rabbit IgG coupled to Alexa® 488 (Molecular Probes, Inc.), affinity-purified goat anti–guinea pig IgG coupled to Alexa® 594 (Molecular Probes, Inc.), or affinity-purified anti–rat IgG coupled to Cy5 were used. As controls, nontransfected cells revealed no labeling for AQP2. Note that in the colocalization analysis of wt-AQP2 and G-AQP2-R187C, the antibodies recognizing wt-AQP2 also recognize G-AQP2-R187C. However, due to the weak expression of G-AQP2-R187C, wt-AQP2 could be well discriminated from G-AQP2-R187C. Finally, preparations were embedded in Vectashield® (Vector Laboratories).

Image acquisition and manipulation

Horizontal and vertical images were obtained with a confocal laser-scanning microscope (MRC 1000; Bio-Rad Laboratories), using a 60× oil lens with NA of 1.4, and with LaserSharp 2000 software (Bio-Rad Laboratories), applying a 3× zoom and an iris of 3. Subsequently, images were imported and merged in Adobe Photoshop® 7.0, and brightness and contrast were adjusted.

Computer-assisted image analysis

To create a semi-objective index for surface versus intracellular expression of the AQP proteins, mean values of integrated optical density (IOD) of surface or intracellular segments were determined using Image Pro Plus analysis software (Media Cybernetics). The basolateral plasma membrane segments were identified by the signal for E-cadherin. Background IOD values were determined within the nuclear area of the particular cell and subtracted from the obtained surface and intracellular IOD values. The ratio of surface to intracellular expression is defined as the corrected IOD of the surface segment divided by the corrected IOD of the intracellular segment. Of eight independent cells from unsaturated images and three segments of the surface and intracellular areas per cell, the mean ratio of surface/intracellular expression ± SEM was determined.

We are grateful to the family bearing the insA mutation for their extensive cooperation.

This work was supported by grants from the Dutch Kidney Foundation (C95.5001), the European Community (FMRX-CT97-0128; BIO4-CT98-0024, QLRT-2000-00778; and QLK3-CT-2001-00987) to P.M.T. Deen and

C.H. van Os; from the Netherlands Organization for Scientific Research to P.M.T. Deen and C.H. van Os (NWO; 902-18-292), and also to E.J. Kamsteeg (NWO; 916.36.122); by a European Molecular Biology Organization fellowship (ALTF-155-2001) to E.J. Kamsteeg; and by grants from the Canadian Institutes of Health Research (MOP-8126) and the Kidney Foundation of Canada to D.G. Bichet.

Submitted: 3 September 2003
Accepted: 27 October 2003

References

Asai, T., M. Kuwahara, H. Kurihara, T. Sakai, Y. Terada, F. Marumo, and S. Sasaki. 2003. Pathogenesis of nephrogenic diabetes insipidus by aquaporin-2 C-terminus mutations. *Kidney Int.* 64:2–10.

Bichet, D.G., M.-F. Arthus, M. Lonergan, G.N. Hendy, A.J. Paradis, T.M. Fujiwara, K. Morgan, M.C. Gregory, W. Rosenthal, A. Didwania, et al. 1993. X-linked nephrogenic diabetes insipidus mutations in North America and the Hopewell hypothesis. *J. Clin. Invest.* 92:1262–1268.

Brewer, C.B., and M.G. Roth. 1991. A single amino acid change in the cytoplasmic domain alters the polarized delivery of influenza virus hemagglutinin. *J. Cell Biol.* 114:413–421.

Brewer, C.B., and M.G. Roth. 1995. Polarized exocytosis in MDCK cells is regulated by phosphorylation. *J. Cell Sci.* 108:789–796.

Casanova, J.E., G. Apodaca, and K.E. Mostov. 1991. An autonomous signal for basolateral sorting in the cytoplasmic domain of the polymeric immunoglobulin receptor. *Cell.* 66:65–75.

Chou, C.L., K.P. Yip, L. Michea, K. Kador, J.D. Ferraris, J.B. Wade, and M.A. Knepper. 2000. Regulation of aquaporin-2 trafficking by vasopressin in renal collecting duct: roles of ryanodine-sensitive Ca^{2+} stores and calmodulin. *J. Biol. Chem.* 275:36839–36846.

Deen, P.M.T., and D. Brown. 2001. Trafficking of native and mutant mammalian MIP proteins. *In* Current Topics in Membranes: Water Channels. S. Hohmann, P. Agre, and S. Nielsen, editors. Academic Press, San Diego, CA. 235–276.

Deen, P.M.T., M.A.J. Verdijk, N.V.A.M. Knoers, B. Wieringa, L.A.H. Monnens, C.H. van Os, and B.A. van Oost. 1994. Requirement of human renal water channel aquaporin-2 for vasopressin-dependent concentration of urine. *Science.* 264:92–95.

Deen, P.M.T., J.P.L. Rijss, S.M. Mulders, R.J. Errington, J. van Baal, and C.H. van Os. 1997. Aquaporin-2 transfection of Madin-Darby canine kidney cells reconstitutes vasopressin-regulated transcellular osmotic water transport. *J. Am. Soc. Nephrol.* 8:1493–1501.

Deen, P.M., B.W. van Balkom, P.J. Savelkoul, E.J. Kamsteeg, M. Van Raak, M.L. Jennings, T.R. Muth, V. Rajendran, and M.J. Caplan. 2002. Aquaporin-2: COOH terminus is necessary but not sufficient for routing to the apical membrane. *Am. J. Physiol. Renal Physiol.* 282:F330–F340.

Folsch, H., H. Ohno, J.S. Bonifacino, and I. Mellman. 1999. A novel clathrin adaptor complex mediates basolateral targeting in polarized epithelial cells. *Cell.* 99:189–198.

Glowatzki, E., G. Fakler, U. Brandle, U. Rexhausen, H.P. Zenner, J.P. Ruppersberg, and B. Fakler. 1995. Subunit-dependent assembly of inward-rectifier K^+ channels. *Proc. R. Soc. Lond. B. Biol. Sci.* 261:251–261.

Heilker, R., M. Spiess, and P. Crottet. 1999. Recognition of sorting signals by clathrin adaptors. *Bioessays.* 21:558–567.

Hoffman, P.W., A. Ravindran, and R.L. Huganir. 1994. Role of phosphorylation in desensitization of acetylcholine receptors expressed in *Xenopus* oocytes. *J. Neurosci.* 14:4185–4195.

Hunziker, W., C. Harter, K. Matter, and I. Mellman. 1991. Basolateral sorting in MDCK cells requires a distinct cytoplasmic domain determinant. *Cell.* 66: 907–920.

Ishibashi, K., S. Sasaki, K. Fushimi, S. Uchida, M. Kuwahara, H. Saito, T. Furukawa, K. Nakajima, Y. Yamaguchi, T. Gojobori, et al. 1994. Molecular cloning and expression of a member of the aquaporin family with permeability to glycerol and urea in addition to water expressed at the basolateral membrane of kidney collecting duct cells. *Proc. Natl. Acad. Sci. USA.* 91: 6269–6273.

Jung, J.S., R.V. Bhat, G.M. Preston, W.B. Guggino, J.M. Baraban, and P. Agre. 1994. Molecular characterization of an aquaporin cDNA from brain: candidate osmoreceptor and regulator of water balance. *Proc. Natl. Acad. Sci. USA.* 91:13052–13056.

Kamsteeg, E.J., and P.M.T. Deen. 2000. Importance of aquaporin-2 expression levels in genotype-phenotype studies in nephrogenic diabetes insipidus. *Am. J. Physiol. Renal Physiol.* 279:F778–F784.

Kamsteeg, E.J., and P.M.T. Deen. 2001. Detection of aquaporin-2 in the plasma membranes of oocytes: a novel isolation method with improved yield and purity. *Biochem. Biophys. Res. Commun.* 282:683–690.

Kamsteeg, E.J., T.A. Wormhoudt, J.P.L. Rijss, C.H. van Os, and P.M.T. Deen. 1999. An impaired routing of wild-type aquaporin-2 after tetramerization with an aquaporin-2 mutant explains dominant nephrogenic diabetes insipidus. *EMBO J.* 18:2394–2400.

Kamsteeg, E.J., I. Heijnen, C.H. van Os, and P.M.T. Deen. 2000. The subcellular localization of an aquaporin-2 tetramer depends on the stoichiometry of phosphorylated and nonphosphorylated monomers. *J. Cell Biol.* 151:919–930.

Katsura, T., C.E. Gustafson, D.A. Ausiello, and D. Brown. 1997. Protein kinase A phosphorylation is involved in regulated exocytosis of aquaporin-2 in transfected LLC-PK1 cells. *Am. J. Physiol.* 272:F817–F822.

Klussmann, E., K. Maric, B. Wiesner, M. Beyermann, and W. Rosenthal. 1999. Protein kinase A anchoring proteins are required for vasopressin-mediated translocation of aquaporin-2 into cell membranes of renal principal cells. *J. Biol. Chem.* 274:4934–4938.

Knauf, F., B. Rogina, Z. Jiang, P.S. Aronson, and S.L. Helfand. 2002. Functional characterization and immunolocalization of the transporter encoded by the life-extending gene Indy. *Proc. Natl. Acad. Sci. USA.* 99:14315–14319.

Koivisto, U.M., A.L. Hubbard, and I. Mellman. 2001. A novel cellular phenotype for familial hypercholesterolemia due to a defect in polarized targeting of LDL receptor. *Cell.* 105:575–585.

Kuwahara, M., K. Iwai, T. Ooeda, T. Igarashi, E. Ogawa, Y. Katsushima, I. Shinbo, S. Uchida, Y. Terada, M.F. Arthus, et al. 2001. Three families with autosomal dominant nephrogenic diabetes insipidus caused by aquaporin-2 mutations in the C-terminus. *Am. J. Hum. Genet.* 69:738–748.

LeBlanc Straceski, J.M., K.T. Montgomery, H. Kissel, L. Murtaugh, P. Tsai, D.C. Ward, K.S. Krauter, and R. Kucherlapati. 1994. Twenty-one polymorphic markers from human chromosome 12 for integration of genetic and physical maps. *Genomics.* 19:341–349.

Madrid, R., S. Le Maout, M.B. Barrault, K. Janvier, S. Benichou, and J. Merot. 2001. Polarized trafficking and surface expression of the AQP4 water channel are coordinated by serial and regulated interactions with different clathrin-adaptor complexes. *EMBO J.* 20:7008–7021.

Marr, N., D.G. Bichet, S. Hoefs, P.J. Savelkoul, I.B.M. Konings, F. De Mattia, M.P.J. Graat, M.F. Arthus, M. Lonergan, T.M. Fujiwara, et al. 2002a. Cell-biologic and functional analyses of five new aquaporin-2 missense mutations that cause recessive nephrogenic diabetes insipidus. *J. Am. Soc. Nephrol.* 13: 2267–2277.

Marr, N., D.G. Bichet, M. Lonergan, M.F. Arthus, N. Jeck, H.W. Seyberth, W. Rosenthal, C.H. van Os, A. Oksche, and P.M.T. Deen. 2002b. Heteroligomerization of an aquaporin-2 mutant with wild-type aquaporin-2 and their misrouting to late endosomes/lysosomes explains dominant nephrogenic diabetes insipidus. *Hum. Mol. Genet.* 11:779–789.

McClure, S.J., and P.J. Robinson. 1996. Dynamin, endocytosis and intracellular signalling (review). *Mol. Membr. Biol.* 13:189–215.

Moyer, B.D., J. Denton, K.H. Karlson, D. Reynolds, S. Wang, J.E. Mickle, M. Milewski, G.R. Cutting, W.B. Guggino, M. Li, and B.A. Stanton. 1999. A PDZ-interacting domain in CFTR is an apical membrane polarization signal. *J. Clin. Invest.* 104:1353–1361.

Mulders, S.M., D.G. Bichet, J.P.L. Rijss, E.J. Kamsteeg, M.F. Arthus, M. Lonergan, M. Fujiwara, K. Morgan, R. Leijendekker, P. van der Sluijs, et al. 1998. An aquaporin-2 water channel mutant which causes autosomal dominant nephrogenic diabetes insipidus is retained in the Golgi complex. *J. Clin. Invest.* 102:57–66.

Neely, J.D., B.M. Christensen, S. Nielsen, and P. Agre. 1999. Heterotetrameric composition of aquaporin-4 water channels. *Biochemistry.* 38:11156–11163.

Nesterov, A., R.E. Carter, T. Sorkina, G.N. Gill, and A. Sorkin. 1999. Inhibition of the receptor-binding function of clathrin adaptor protein AP-2 by dominant-negative mutant μ2 subunit and its effects on endocytosis. *EMBO J.* 18:2489–2499.

Nielsen, S., S.R. Digiovanni, E.I. Christensen, M.A. Knepper, and H.W. Harris. 1993. Cellular and subcellular immunolocalization of vasopressin-regulated water channel in rat kidney. *Proc. Natl. Acad. Sci. USA.* 90:11663–11667.

Ohno, H., M.C. Fournier, G. Poy, and J.S. Bonifacino. 1996. Structural determinants of interaction of tyrosine-based sorting signals with the adaptor medium chains. *J. Biol. Chem.* 271:29009–29015.

Prill, V., L. Lehmann, K. von Figura, and C. Peters. 1993. The cytoplasmic tail of

lysosomal acid phosphatase contains overlapping but distinct signals for basolateral sorting and rapid internalization in polarized MDCK cells. *EMBO J.* 12:2181–2193.

Robinson, M.S., and J.S. Bonifacino. 2001. Adaptor-related proteins. *Curr. Opin. Cell Biol.* 13:444–453.

Sandoval, I.V., and O. Bakke. 1994. Targeting of membrane proteins to endosomes and lysosomes. *Trends Cell Biol.* 4:292–297.

Scheiffele, P., J. Peranen, and K. Simons. 1995. N-glycans as apical sorting signals in epithelial cells. *Nature.* 378:96–98.

Simmen, T., S. Honing, A. Icking, R. Tikkanen, and W. Hunziker. 2002. AP-4 binds basolateral signals and participates in basolateral sorting in epithelial MDCK cells. *Nat. Cell Biol.* 4:154–159.

Simons, K., and E. Ikonen. 1997. Functional rafts in cell membranes. *Nature.* 387: 569–572.

Smith, B.L., and P. Agre. 1991. Erythrocyte M_r 28,000 transmembrane protein exists as a multisubunit oligomer similar to channel proteins. *J. Biol. Chem.* 266:6407–6415.

Tinker, A., Y.N. Jan, and L.Y. Jan. 1996. Regions responsible for the assembly of inwardly rectifying potassium channels. *Cell.* 87:857–868.

van Balkom, B.W., P.J.M. Savelkoul, D. Markovich, E. Hofman, S. Nielsen, P. van der Sluijs, and P.M.T. Deen. 2002. The role of putative phosphorylation sites in the targeting and shuttling of the aquaporin-2 water channel. *J. Biol. Chem.* 277:41473–41479.

Verkarre, V., J.C. Fournet, P. de Lonlay, M.S. Gross-Morand, M. Devillers, J. Rahier, F. Brunelle, J.J. Robert, C. Nihoul-Fekute, J.M. Saudubray, and C. Junien. 1998. Paternal mutation of the sulfonylurea receptor (SUR1) gene and maternal loss of 11p15 imprinted genes lead to persistent hyperinsulinism in focal adenomatous hyperplasia. *J. Clin. Invest.* 102:1286–1291.

Wehrle-Haller, B., and B.A. Imhof. 2001. Stem cell factor presentation to c-Kit. Identification of a basolateral targeting domain. *J. Biol. Chem.* 276:12667–12674.

Wild, K., and J. Paysan. 2002. Single amino acid residue influences the distribution pattern of an inwardly rectifying potassium channel in polarized cells. *Cell Tissue Res.* 307:47–55.

Xu, Z.C., Y. Yang, and S.C. Hebert. 1996. Phosphorylation of the ATP-sensitive, inwardly rectifying K^+ channel, ROMK, by cyclic AMP-dependent protein kinase. *J. Biol. Chem.* 271:9313–9319.